

Aharonov-Casher Effect in Wigner Crystal Exchange Interactions

Yaroslav Tserkovnyak¹ and Markus Kindermann²

¹*Department of Physics and Astronomy, University of California, Los Angeles, California 90095, USA*

²*School of Physics, Georgia Institute of Technology, Atlanta, Georgia 30332, USA*

(Dated: April 28, 2022)

We theoretically study the effects of spin-orbit coupling on spin exchange in a low-density Wigner crystal. In addition to the familiar antiferromagnetic Heisenberg exchange, we find general anisotropic interactions in spin space if the exchange paths allowed by the crystal structure form loops in real space. In particular, the two-electron exchange interaction can acquire ferromagnetic character.

PACS numbers: 73.21.Hb, 75.10.Pq, 75.30.Et, 71.70.Ej

In the absence of spin-orbit coupling, the two-electron exchange interaction takes the Heisenberg form, $J\mathbf{S}_1 \cdot \mathbf{S}_2$, as a consequence of spin-rotational symmetry. Because typically the lowest energy orbital wave functions are symmetric under particle interchange, the spin exchange is generically antiferromagnetic ($J > 0$), as a consequence of the Pauli principle. This statement has been established rigorously for one-dimensional (1D) many-electron systems with velocity- and spin-independent interactions [1]. The spin-orbit interaction (SOI), however, has long been known to modify the Heisenberg form of the exchange Hamiltonian by, e.g., effectively canting the participating spins. The resulting Dzyaloshinsky-Moriya (DM) interaction [2] of the form $\mathbf{D} \cdot (\mathbf{S}_1 \times \mathbf{S}_2)$, with some structure-dependent vector \mathbf{D} , was initially studied in the context of weak ferromagnetism in materials that otherwise were expected to be antiferromagnetic, but has since been appreciated in many other contexts.

This paper continues the recent discussion of the SOI in mesoscopic and Wigner-crystal exchange processes [3, 4, 5, 6]. For definiteness, we focus our attention on clean strongly-interacting quasi-1D systems. Two-electron as well as ring exchange interactions in single- and double-row quasi-1D systems without SOI were extensively discussed in Refs. [7, 8]. We show that the SOI qualitatively enriches the electronic behavior in 1D by causing anisotropies in the exchange Hamiltonian. Our calculation is performed using the path integral-based instanton picture of particle exchange [8, 9]. In the low-density limit, $b \ll a_B$, where $b = n^{-1}$ is the average inter-electron separation and $a_B = \varepsilon\hbar^2/me^2$ is the Bohr radius, the dominant electron paths follow classical trajectories in the inverted potential that they are subject to. In this limit, the SOI is naturally captured by the purely geometric SU(2) transformations that the electron spins undergo along their exchange paths [10]. See Fig. 1 for a schematic. We thus explore the non-Abelian Aharonov-Casher [11] variant of physics whose Aharonov-Bohm counterpart was studied extensively in Ref. [12].

To illustrate our approach and the key findings, we first consider two spin-1/2 electrons confined to move

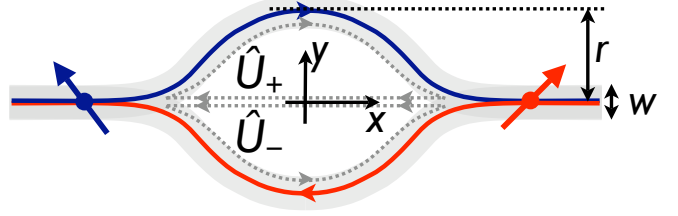


FIG. 1: (Color online) Electrons confined to move closely to the x axis undergo a geometric (Aharonov-Casher) spin transformation as they exchange their positions by tunneling through the mutual Coulomb repulsion barrier. The shaded area marks the transverse confinement of width w . As the electrons exchange their positions, they deviate from the x axis by the distance $r \sim w(w/a_B)^{1/3} \gg w$. Sketched here are the classical exchange trajectories in the instanton picture, which follow the rim of the inverted center-of-mass potential. \hat{U}_{\pm} is the SOI SU(2) transformation starting at the origin of the xy coordinate system, moving to the left, then (counter)clockwise along the upper (lower) rim and back. The total area enclosed by the two trajectories is $A \sim r^2$.

in the xy plane, subject to the two-dimensional (2D) effective-mass Hamiltonian (denoting by hats the spin matrix structure):

$$\hat{H} = \sum_{j=1,2} \left[\frac{1}{2m} \left(-i\hbar\nabla_j + \hat{\mathbf{A}}_j \right)^2 + V_j \right] + U_{12}. \quad (1)$$

Here, $\nabla_j = (\partial_{x_j}, \partial_{y_j})$ and $\mathbf{A}_j = \hat{\mathbf{A}}(\mathbf{r}_j) = (\hat{A}_x, \hat{A}_y)$ is the two-component 2×2 vector potential, which can be expanded in the basis of the three Pauli matrices $(\hat{\sigma}_x, \hat{\sigma}_y, \hat{\sigma}_z) \equiv \hat{\boldsymbol{\sigma}}$. The SU(2) vector potential $\hat{\mathbf{A}}$ describes the SOI. The Pauli equation for electrons in vacuum, for example, has $\hat{\mathbf{A}} \propto \nabla V \times \hat{\boldsymbol{\sigma}}$, while in 2D (solid-state) electron systems with asymmetric confining potential along the z axis, the SOI is usually dominated by the so-called Rashba interaction of the form:

$$\hat{\mathbf{A}} = \alpha \mathbf{z} \times \hat{\boldsymbol{\sigma}}. \quad (2)$$

Further, $U_{12} = U(\mathbf{r}_1 - \mathbf{r}_2)$ is the effective two-particle repulsion and $V_j = V(\mathbf{r}_j)$ is the 2D potential that ensures

lateral confinement close to the x axis. The two-electron exchange then becomes a quasi-1D scattering problem: In the center-of-mass reference frame, electrons are incident from opposite directions and are scattering near the origin, $\Delta\mathbf{r} = \mathbf{r}_1 - \mathbf{r}_2 \sim 0$. The electron transmission through their mutual repulsion potential $U(\Delta\mathbf{r})$ in our low-density limit of strong repulsion is well approximated by WKB tunneling.

We start by assuming a homogeneous SOI of the form (2). In the strictly one-dimensional limit, when the lateral motion along the y direction can be completely neglected, it is possible to gauge out the SOI by the unitary transformation

$$\hat{W}(x) = e^{-(i/\hbar)x\hat{A}_x}. \quad (3)$$

When applied to each electron separately, this gauge transformation removes the vector potential $\hat{\mathbf{A}}$ from the Hamiltonian. It is, however, not possible to generalize this to 2D, since \hat{A}_x and \hat{A}_y in general do not commute. We, nevertheless, choose to transform our 2D Hamiltonian (1) as $\hat{H} \rightarrow \hat{W}^\dagger \hat{H} \hat{W}$. When the electrons are sufficiently distant from each other and they stay close to $y = 0$ due to the $V(y)$ confinement, the transformation (3) then does remove the SOI from the problem. It is only during the short time intervals when the electrons tunnel through each other that they deviate appreciably from the x axis and undergo an additional SOI-induced spin transformation (see Fig. 1). It is this remnant spin precession that the gauge (3) allows us to focus on. To simplify our discussion, we assume that the spin precession length $l_{\text{so}} = \pi\hbar/\alpha$ is much longer than the width $w = \sqrt{\hbar}/m\omega$ of the wire (assuming quadratic lateral confinement $V = m\omega^2 y^2/2$), while the Bohr radius a_B is much shorter than w : $a_B \ll w \ll l_{\text{so}}$. The average separation between electrons b is, furthermore, taken to be large enough so that the problem may be viewed as effectively 1D, although this is not essential.

Before proceeding, it is instructive to recall how one constructs the exchange Hamiltonian in the low-density limit without SOI using the instanton method. The strength of the exchange is parametrized by a positive real-valued parameter J , which is determined by the Euclidian action S_E along the minimal-action path exchanging two electrons [8, 9]:

$$J = \beta\hbar\omega_0 \sqrt{\frac{S_E}{2\pi\hbar}} e^{-S_E/\hbar}, \quad (4)$$

where ω_0 is the characteristic attempt frequency (corresponding to the effective electron confinement along the wire) and β is a numerical prefactor of order unity. The classical minimal action path corresponds approximately to the rim of the inverted repulsion potential $U_E(\Delta\mathbf{r}) = V(\Delta y)/2 + U(\Delta\mathbf{r})$ (again assuming quadratic

confinement) in the center-of-mass frame:

$$S_E \approx \int_{-b}^b dl \sqrt{2m^*U_E(l)}. \quad (5)$$

J is thus essentially the WKB tunneling amplitude for a particle with the reduced mass $m^* = m/2$ through the potential barrier U_E along the classical trajectory parametrized by l . The authors of Ref. [8] performed a detailed study of the Euclidian action in quasi-1D wires, obtaining in the regime considered here (namely, $a_B \ll w, r \ll b$):

$$S_E/\hbar \approx \eta\sqrt{b/a_B} - \kappa(w/a_B)^{2/3}, \quad (6)$$

where η and κ are numerical prefactors of order unity. The first term on the right-hand side is the action for the head-on tunneling of electrons and the second term is its reduction due to lateral excursions that allow electrons to avoid each other, as sketched in Fig. 1.

In the absence of the SOI, J parametrizes the usual antiferromagnetic coupling between the two spins [8]:

$$\hat{H}_{\text{AF}} = J(\hat{\mathbf{1}} \otimes \hat{\mathbf{1}} + \hat{\boldsymbol{\sigma}} \otimes \hat{\boldsymbol{\sigma}}), \quad (7)$$

making the convention that the left (right) operator in a direct product $\hat{L} \otimes \hat{R}$ acts on the left (right) spin. Note that the operator $\hat{X} = (\hat{\mathbf{1}} \otimes \hat{\mathbf{1}} + \hat{\boldsymbol{\sigma}} \otimes \hat{\boldsymbol{\sigma}})/2$ simply exchanges the spins: $\hat{X}|s_1, s_2\rangle = |s_2, s_1\rangle$, where $|s_1, s_2\rangle$ is the spinor wave function with s_1 and s_2 corresponding to the left and the right spin, respectively. In the case of multiple exchange trajectories, J stands for the sum of all contributions.

We now include SOI effects in the above approach. During their exchange, two electrons j that are moving along paths \mathcal{C}_j , undergo the path-dependent SU(2) transformations [10]

$$\hat{U}_j = T_{\mathcal{C}_j} e^{-(i/\hbar)\oint_{\mathcal{C}_j} d\mathbf{r} \cdot \hat{\mathbf{A}}}, \quad (8)$$

where $T_{\mathcal{C}_j}$ is the contour-ordering operator and the integral runs over the classical exchange paths closed back along the x axis, as shown in Fig. 1. The integration thus starts and ends at the initial electron positions, which is necessary because of our initial unitary transformation (3). We choose the point where the two electrons pass each other to be at $x = 0$, see Fig. 1, and integrate counterclockwise along the lower classical exchange trajectory and clockwise along the upper path. The SOI is assumed to be weak in comparison to the interparticle repulsion, such that the effect of the spin dynamics on the instanton orbital trajectories may be neglected.

The effective spin Hamiltonian is finally obtained in the form:

$$\hat{H}_s = \frac{J}{2} \left(\hat{U}_+^\dagger \otimes \hat{U}_- + \hat{U}_-^\dagger \otimes \hat{U}_+ \right) (\hat{\mathbf{1}} \otimes \hat{\mathbf{1}} + \hat{\boldsymbol{\sigma}} \otimes \hat{\boldsymbol{\sigma}}). \quad (9)$$

The operator $(\hat{U}_-^\dagger \otimes \hat{U}_+) \hat{X}$ implements the spin transformation along the clockwise exchange trajectory, when the left electron deviates from $y = 0$ toward positive y , moving to the right, while the right electron is correspondingly pushed toward negative y , moving to the left. The other term $\hat{U}_+^\dagger \otimes \hat{U}_-$ accounts for the counterclockwise exchange path. The Hamiltonian is verified to be Hermitian through the identity $\hat{X}(\hat{U}_+ \otimes \hat{U}_-^\dagger) = (\hat{U}_-^\dagger \otimes \hat{U}_+) \hat{X}$. Note that if the electron exchange occurs at $x = x_0$ instead of $x = 0$, as in Fig. 1, the above Hamiltonian has to be rotated by $\hat{W}(x_0)$: $\hat{H}_s \rightarrow \hat{W}^\dagger(x_0) \hat{H}_s \hat{W}(x_0)$, with \hat{W} acting on both spins.

We now employ Eq. (9) to calculate the spin exchange coupling in the presence of the SOI, Eq. (1). Parametrizing $\hat{U}_\pm = u_\pm - i\mathbf{u}_\pm \cdot \hat{\boldsymbol{\sigma}}$ with real-valued scalars u_\pm and vectors \mathbf{u}_\pm , such that $u_\pm^2 + \mathbf{u}_\pm^2 = 1$, the Hamiltonian (9) acquires the form (omitting a constant offset):

$$\begin{aligned} \hat{H}_s/J = & (u_+u_- - \mathbf{u}_+ \cdot \mathbf{u}_-) \hat{\boldsymbol{\sigma}}_1 \cdot \hat{\boldsymbol{\sigma}}_2 + \mathbf{d} \cdot (\hat{\boldsymbol{\sigma}}_1 \times \hat{\boldsymbol{\sigma}}_2) \\ & + 2(\mathbf{a} \cdot \hat{\boldsymbol{\sigma}}_1)(\mathbf{a} \cdot \hat{\boldsymbol{\sigma}}_2) - 2(\mathbf{b} \cdot \hat{\boldsymbol{\sigma}}_1)(\mathbf{b} \cdot \hat{\boldsymbol{\sigma}}_2), \end{aligned} \quad (10)$$

where $\mathbf{d} = u_+\mathbf{u}_- + u_-\mathbf{u}_+$ parametrizes DM, $\mathbf{a} = (\mathbf{u}_+ + \mathbf{u}_-)/2$ Ising antiferromagnetic, and $\mathbf{b} = (\mathbf{u}_+ - \mathbf{u}_-)/2$ Ising ferromagnetic interactions. The operators $\hat{\boldsymbol{\sigma}}_1$ and $\hat{\boldsymbol{\sigma}}_2$ act on the left and right spin, respectively.

Specializing now to the Rashba case (2) and expanding the transformation matrices in $\gamma = \sqrt{A}(\alpha/\hbar)$ (where A is the total area of the loop formed by the two classical trajectories in Fig. 1), we have [10]:

$$\hat{U}_\pm = 1 \pm i\gamma^2 \hat{\sigma}_z + i\gamma^3 \mathbf{v}_\pm \cdot \hat{\boldsymbol{\sigma}} + \mathcal{O}(\gamma^4). \quad (11)$$

Since the cubic-order in γ contribution to \hat{U}_\pm depends on the exact shape of the exchange loop, we parametrized it by the dimensionless spin-space vectors \mathbf{v}_\pm . The same is true also of the higher-order terms. Substituting the expansion (11) into Eq. (10) gives:

$$\hat{H}_s^{\text{pert}}/J = \hat{\boldsymbol{\sigma}}_1 \cdot \hat{\boldsymbol{\sigma}}_2 - \gamma^3 \mathbf{v} \cdot (\hat{\boldsymbol{\sigma}}_1 \times \hat{\boldsymbol{\sigma}}_2) - 2\gamma^4 \hat{\sigma}_{1z} \hat{\sigma}_{2z}, \quad (12)$$

where $\mathbf{v} = \mathbf{v}_+ + \mathbf{v}_-$. In addition to the leading anti-ferromagnetic coupling, we find a DM interaction [2] at order γ^3 and a ferromagnetic Ising coupling along the z axis at $\mathcal{O}(\gamma^4)$. In the approximation (12), we retained only the leading in γ terms separately for Heisenberg, DM, and Ising interactions. If the wire is mirror symmetric with respect to the xz plane, we have $u_+ = u_-$ and $\mathbf{u}_- = -\hat{M}\mathbf{u}_+$, where \hat{M} stands for the mirror image, so that $\mathbf{u}_+ + \mathbf{u}_- = \mathbf{u}_+ - \hat{M}\mathbf{u}_+ \propto \mathbf{y}$. This means, in particular, that $\mathbf{d} \propto \mathbf{y}$ in Eq. (10) and the DM interaction $\hat{H}_{\text{DM}} \propto \mathbf{y} \cdot (\hat{\boldsymbol{\sigma}}_1 \times \hat{\boldsymbol{\sigma}}_2)$ is of the general form allowed by the mirror symmetry, to all orders in γ . Furthermore, a Rashba system is mirror-symmetric with respect to the xy plane (combined with flipping $\alpha \rightarrow -\alpha$). This constrains the DM coupling to be odd and the Heisenberg and Ising terms even in α , in accordance with Eq. (12).

A ferromagnetic Ising coupling of the form $\hat{\sigma}_{1z} \hat{\sigma}_{2z}$ is also expected as a consequence of correlated orbital quantum fluctuations, which produce van der Waals type spin interactions via SOI [6]. A form of the exchange interaction similar to our Eq. (12), consisting of the Heisenberg, Ising, and DM pieces has been reported before in Refs. [3, 4]. An analogous result was also found for the RKKY interaction mediated by itinerant electrons in the presence of the Rashba SOI [5]. In contrast to our Eq. (10), however, these earlier Refs. [3, 4, 5, 6] predicted a spin exchange Hamiltonian of the form:

$$\hat{H}_s^{(0)} = J \hat{\boldsymbol{\sigma}}_1 \cdot \hat{\boldsymbol{\sigma}}_2 + \Upsilon \mathbf{n} \cdot (\hat{\boldsymbol{\sigma}}_1 \times \hat{\boldsymbol{\sigma}}_2) + \Gamma (\mathbf{n} \cdot \hat{\boldsymbol{\sigma}}) (\mathbf{n} \cdot \hat{\boldsymbol{\sigma}}), \quad (13)$$

parametrized by a single vector \mathbf{n} . This stemmed from a hidden SU(2) symmetry of the exchange Hamiltonian in Refs. [3, 5] (when the Hamiltonian can be written as a Heisenberg exchange between canted spins) and from a spin-rotational symmetry around \mathbf{n} in Ref. [4]. Such symmetries are not assumed in our calculation based on Eq. (9).

To compare our Eq. (10) to the earlier prediction (13), we distinguish two effects of the SOI on the exchange Hamiltonian [6]. First, the SO coupling cants the participating spins through a spin rotation along the exchange path. We have already gauged out the main part of that rotation by means of our transformation \hat{W} , Eq. (3), but deviations of the exchange paths from the x axis ($y = 0$) add another piece, contributing to \hat{U}_\pm . A canting of two spins that participate in the usual Heisenberg exchange [3, 5, 6] by a rotation angle θ around the direction \mathbf{n} ,

$$\hat{H}_{\mathbf{n}}/J = \left(\hat{V}_1 \hat{\boldsymbol{\sigma}}_1 \hat{V}_1^\dagger \right) \cdot \left(\hat{V}_2 \hat{\boldsymbol{\sigma}}_2 \hat{V}_2^\dagger \right), \quad (14)$$

where $\hat{V}_j = e^{-i\mathbf{n} \cdot \hat{\boldsymbol{\sigma}}_j \theta/2}$, produces an exchange Hamiltonian:

$$\begin{aligned} \hat{H}_{\mathbf{n}}/J = & \cos 2\theta \hat{\boldsymbol{\sigma}}_1 \cdot \hat{\boldsymbol{\sigma}}_2 - \sin 2\theta \mathbf{n} \cdot (\hat{\boldsymbol{\sigma}}_1 \times \hat{\boldsymbol{\sigma}}_2) \\ & + (1 - \cos 2\theta) (\mathbf{n} \cdot \hat{\boldsymbol{\sigma}}_1) (\mathbf{n} \cdot \hat{\boldsymbol{\sigma}}_2), \end{aligned} \quad (15)$$

that looks anisotropic and similar to Eq. (13). However, as was already pointed out in Refs. [6, 13], $\hat{H}_{\mathbf{n}}$ has the same eigenvalues as the isotropic Heisenberg exchange Hamiltonian (7). A mere canting of two spins should thus not be considered a real anisotropy, although the resulting Hamiltonian (15) has a DM and an Ising piece.

Our exchange geometry has a two-dimensional character with two different exchange paths corresponding to different transformations \hat{U}_+ and \hat{U}_- . This results in an exchange Hamiltonian \hat{H}_s whose eigenvalues differ from those of \hat{H}_{AF} , Eq. (7). In order to quantify this second and more interesting effect of the SOI, and to disentangle it from the effects of a mere canting of the participating spins, Eq. (14), we bring the exchange Hamiltonian \hat{H}_s into a standard form through local spin rotations. To this end, we first rewrite \hat{H}_s , Eq. (10), as:

$$\hat{H}_s/J = \hat{\boldsymbol{\sigma}}_1 \vec{h} \hat{\boldsymbol{\sigma}}_2, \quad (16)$$

in terms of a real-valued 3×3 tensor \vec{h} . Through a singular-value decomposition (SVD), we then bring \vec{h} into the form $\vec{h} = \hat{R}\hat{D}\hat{T}^T$, with rotation matrices $\hat{R}, \hat{T} \in \text{SO}(3)$ and a real-valued diagonal matrix \hat{D} . The diagonal matrices \hat{D} are the desired standardized representation of exchange Hamiltonians. We find for our exchange Hamiltonian Eq. (10) that

$$D_{xx} = 1, \quad D_{yy} = 1, \quad D_{zz} = u_+u_- + \mathbf{u}_+ \cdot \mathbf{u}_-. \quad (17)$$

The sign of D_{zz} determines whether the exchange interaction in the rotated spin coordinates has antiferromagnetic ($u_+u_- + \mathbf{u}_+ \cdot \mathbf{u}_- > 0$) or ferromagnetic ($u_+u_- + \mathbf{u}_+ \cdot \mathbf{u}_- < 0$) character: Rotations by π around the coordinate z -axis can be used to flip the signs of D_{xx} and D_{yy} such that all entries of \vec{D} have the same sign as D_{zz} .

Note that our exchange Hamiltonian (9) always has a pair of degenerate singular values $|D_{jj}|$, for any \hat{U}_+ and \hat{U}_- , realizing an XXZ model in rotated spin coordinates. This general statement is easiest understood by expressing the square of the Hamiltonian (9),

$$\frac{\hat{H}_s^2}{J^2} = \frac{1}{4} \left(\hat{U}_+^\dagger \hat{U}_- \otimes \hat{U}_- \hat{U}_+^\dagger + \hat{U}_-^\dagger \hat{U}_+ \otimes \hat{U}_+ \hat{U}_-^\dagger \right) + \frac{1}{2}, \quad (18)$$

in a basis where the transformations $\hat{U}_+^\dagger \hat{U}_-$ acting on the left spin and $\hat{U}_- \hat{U}_+^\dagger$ acting on the right spin are diagonal. The only spin operator occurring in the expression for \hat{H}_s^2 is then $\hat{\sigma}_{1z} \hat{\sigma}_{2z}$. Evidently, \hat{H}_s^2 is severely constrained: it has an Ising form in proper coordinates. This allows us to draw conclusions about \hat{H}_s itself, after writing it in the general form $\hat{H}_s/J = \hat{\sigma}_1 \vec{h} \hat{\sigma}_2 + c$, where we restored the constant c that was omitted in Eq. (10). In the spin basis where \vec{h} is diagonal also the tensor representing \hat{H}_s^2 is diagonal and, according to Eq. (18), only one of its elements is nonzero. Straightforward algebra then shows that this implies $D_{xx}^2 = D_{yy}^2$, so that $|D_{xx}| = |D_{yy}|$ (up to a permutation between three cartesian axes).

We give also the explicit form of the transformations \hat{R} and \hat{T} for Rashba SOI with mirror symmetry \hat{M} . In that case, \hat{R} and \hat{T} rotate the spins around the y axis by the angles θ_R and θ_T , respectively, where

$$\theta_R = \arctan \frac{u_{+x}u_{+y} + u_{+u_{+z}} - \frac{\pi}{2} \text{sgn}(u_{+y}u_{+z} - u_{+u_{+x}})}{u_{+y}u_{+z} - u_{+u_{+x}}}, \quad (19)$$

and θ_T is obtained from θ_R by the substitution $\mathbf{u}_+ \rightarrow \hat{M}\mathbf{u}_+$.

We are now ready to compare the exchange Hamiltonian $\hat{H}_s^{(0)}$, Eq. (13), obtained in Refs. [3, 4, 5, 6] to our \hat{H}_s , Eq. (10). Representing $\hat{H}_s^{(0)}$ by a corresponding tensor $\vec{h}^{(0)}$, we find that also $\vec{h}^{(0)}$ has at least one pair of identical singular values. $\hat{H}_s^{(0)}$ thus realizes an XXZ model in a rotated spin basis, just as our \hat{H}_s , Eq. (10).

Eq. (10) has been derived in the strongly interacting limit under the assumption that only a single pair of (mutually time-reversed) exchange paths contributes. For the case that the inverted repulsion potential has more than one saddle point, one finds that the exchange Hamiltonian after a SVD in general will take the form of an XYZ model. The same holds true if the orbital dynamics in the x direction allows particle exchanges at a variety of locations $x = x_0$. The resulting exchange Hamiltonian $\hat{H}_s \rightarrow \hat{W}^\dagger(x_0)\hat{H}_s\hat{W}(x_0)$ averaged over x_0 may then also realize a Heisenberg exchange with two independent anisotropy axes, an XYZ model.

Let us turn briefly to many-electron systems that are effectively one-dimensional through the confining potential $V(y)$. In the absence of SOI, the generic antiferromagnetic exchange Hamiltonian \hat{H}_{AF} there results in the expected Luttinger-liquid behavior at low energies [14]. Deviations from \hat{H}_{AF} , however, can have profound consequences. In Refs. [15], for example, spin-charge separation described by a new universality class has been found for a 1D Bose gas with ferromagnetic Heisenberg exchange. One may thus expect important implications of our Eq. (10) for strongly interacting quantum wires. We leave a detailed analysis of this topic for future research and make only a few general remarks here.

It was shown in Refs. [8] that the effects of the coupling of the exchanging electrons to surrounding electrons in a many-electron system may be systematically included in the instanton approach employed above. It has been found that in typical limits this produces merely small corrections. In a translationally invariant wire without SOI, the two-electron exchange Hamiltonian then carries over to the many-electron system, $\hat{H}_s^{\text{wire}} = \hat{H}_s$. With SOI, however, that is no longer true, as the Hamiltonian \hat{H}_s^{wire} acquires a position dependence through our gauge transformation (3): $\hat{H}_s^{\text{wire}} = \hat{W}^\dagger \hat{H}_s \hat{W}$. The pairwise exchange interaction thus becomes x -dependent (unless \hat{H}_s is invariant under \hat{W}), which couples the orbital motion to the spin dynamics. We furthermore remark that even if \hat{W} has no effect on \hat{H}_s^{wire} , one generally cannot bring the exchange Hamiltonians into a diagonal form for all pairs of neighboring spins simultaneously by a proper choice of spin bases. The rotations in the above SVD decomposition are in general incompatible for consecutive spin pairs.

In conclusion, we have analyzed spin exchange in effectively one-dimensional interacting electron systems at low density. In a two-electron system, the resulting exchange Hamiltonian can be brought into the form of an anisotropic Heisenberg model. The model can have both antiferromagnetic and ferromagnetic character. We have discussed general conditions for the degree of anisotropy of the resulting exchange. Both XXZ and XYZ models may be realized. Our results may have profound implications for interacting many-electron systems in one dimension.

We are grateful to Shimul Akhanjee for stimulating discussions. This work was supported in part by the Alfred P. Sloan Foundation.

-
- [1] E. Lieb and D. Mattis, Phys. Rev. **125**, 164 (1962).
 [2] I. Dzyaloshinsky, J. Phys. Chem. Solids **4**, 241 (1958); T. Moriya, Phys. Rev. **120**, 91 (1960).
 [3] K. V. Kavokin, Phys. Rev. B **64**, 075305 (2001); *ibid.* **69**, 075302 (2004).
 [4] D. Stepanenko, N. E. Bonesteel, D. P. DiVincenzo, G. Burkard, and D. Loss, Phys. Rev. B **68**, 115306 (2003).
 [5] H. Imamura, P. Bruno, and Y. Utsumi, Phys. Rev. B **69**, 121303(R) (2004).
 [6] S. Gangadharaiyah, J. Sun, and O. A. Starykh, Phys. Rev. Lett. **100**, 156402 (2008).
 [7] K. A. Matveev, Phys. Rev. Lett. **92**, 106801 (2004).
 [8] A. D. Klironomos, R. R. Ramazashvili, and K. A. Matveev, Phys. Rev. B **72**, 195343 (2005); A. D. Klironomos, J. S. Meyer, and K. A. Matveev, Europhys. Lett. **74**, 679 (2006); A. D. Klironomos, J. S. Meyer, T. Hikihara, and K. A. Matveev, Phys. Rev. B **76**, 075302 (2007).
 [9] K. Voelker and S. Chakravarty, Phys. Rev. B **64**, 235125 (2001).
 [10] Y. Tserkovnyak and A. Brataas, Phys. Rev. B **76**, 155326 (2007); Y. Tserkovnyak and S. Akhanjee, arXiv:0804.2706.
 [11] Y. Aharonov and A. Casher, Phys. Rev. Lett. **53**, 319 (1984).
 [12] T. Okamoto and S. Kawaji, Phys. Rev. B **57**, 9097 (1998).
 [13] L. Shekhtman, O. Entin-Wohlman, and A. Aharony, Phys. Rev. Lett. **69**, 836 (1992).
 [14] K. A. Matveev, A. Furusaki, and L. I. Glazman, Phys. Rev. Lett. **98**, 096403 (2007).
 [15] M. B. Zvonarev, V. V. Cheianov, and T. Giamarchi, Phys. Rev. Lett. **99**, 240404 (2007); S. Akhanjee and Y. Tserkovnyak, Phys. Rev. B **76**, 140408(R) (2007).